

# Spin-dependent energy relaxation inside a quantum dot

Toshimasa Fujisawa<sup>a,\*</sup>, Yasuhiro Tokura<sup>a</sup>, David G. Austing<sup>a</sup>, Yoshiro Hirayama<sup>a,b</sup>, and Seigo Tarucha<sup>a,c,d</sup>

<sup>a</sup>NTT Basic Research Laboratories, NTT Corporation,

3-1 Morinosato-Wakamiya, Atsugi, 243-0198, Japan

<sup>b</sup>CREST, 4-1-8 Honmachi, Kawaguchi, 331-0012, Japan

<sup>c</sup>University of Tokyo, Bunkyo-ku, Tokyo, 113-0033, Japan

<sup>d</sup>ERATO Mesoscopic Correlation Project,

3-1 Morinosato-Wakamiya, Atsugi, 243-0198, Japan

We employ pulse excitation measurements in order to investigate spin-dependent energy relaxation inside a quantum dot. A fast pulse signal is applied to a gate electrode in order to excite a quantum dot, and the induced transient current is analyzed in terms of energy relaxation. We describe transient current measurements on a lateral quantum dot, in which the tunneling rates are controllable with gate voltages, and on a vertical quantum dot, in which the total number of electrons and total spin can be well identified. The spin-conservation rule during energy relaxation is clearly identified.

PACS numbers: 73.61.Ey, 73.23.Hk, 85.30.Vw

Keywords: quantum dot, electron spin, energy relaxation, Coulomb blockade.

\*)corresponding author, e-mail: fujisawa@will.brl.ntt.co.jp, fax: +81-46-240-4727.

## I. INTRODUCTION

Semiconductor quantum dots (QDs), in which electrons occupy discrete energy states, show various spin-related phenomena, including spin degeneracy, exchange interaction, spin blockade, and Kondo physics [1-5]. Transitions between dot states, which are responsible for the coupling to the dot environment, should strongly reflect the characteristics of the states in close analogy with selection rules for absorption and emission processes in real atoms. The energy relaxation process, which is a spontaneous transition from an excited state (ES) to a ground state (GS), is one of the important characteristics of spin dynamics. Electronic states in a solid can easily couple to the lattice environment, i.e. phonons [6,7]. Theory predicts that the energy relaxation time of an ES in a QD is of the order of nanoseconds if the transition is accompanied by acoustic phonon emission, provided the spin is neglected [8]. In contrast, it should be extremely long if the transition involves a spin flip [9]. Spin conservation during a transition is a selection rule for artificial atoms.

In order to investigate spin conservation experimentally, we perform pulse excitation measurements, in which a transient current through an ES reflects the energy relaxation time in the QD. We describe in detail the amplitude of the transient current, and discuss measurements on a lateral QD, in which the tunneling rate of two tunneling barriers can be adjusted, and on a vertical QD, in which total number of electrons,  $N$ , and total spin,  $S$  can be readily identified. A spin conservation rule during relaxation is clearly demonstrated.

## II. TRANSIENT CURRENT SPECTRUM

In order to investigate energy relaxation from an ES to a GS, we use a pulse excitation to push the system out of equilibrium. We apply a pulse signal to the gate electrode to modulate the electrostatic potential of the dot (see Fig. 1), and measure the averaged transient current in the following way. When the pulse is in the low-phase (duration  $t_l$ ), both the ES and the GS for a particular number of electrons are located well above the chemical potential of the contacts,  $\mu_L$  and  $\mu_R$ . After a sufficiently long time,  $t_l$ , an electron is depleted from these states [Fig. 1(b)]. When the pulse is turned to the high-phase (duration  $t_h$ ), the potential of the dot is lowered by an energy  $\alpha V_p$  ( $\alpha$  is the conversion factor from gate voltage to energy, and  $V_p$  is the amplitude of the pulse). We consider the case that the excitation energy  $\alpha V_p$  is larger than the energy spacing between the GS and ES, but smaller than the addition energy of the QD. Thus, only one electron can enter either the GS or the ES. If the conditions are adjusted so that only the ES is located in the transport window [Fig. 1(c)], transport through the ES continues until the GS becomes occupied. First, an electron tunnels into the ES or the GS with a probability ratio,  $j_{L,e} : j_{L,g}$ . If an electron is injected into the ES, it can relax to the GS, or tunnel out to the right lead to give a net current. The transport is transient, being blocked once the GS is occupied. We chose asymmetric barriers,  $j_L \gg j_R$ , such that an electron can stay in the ES for a long time. Thus, the decay time,  $\tau$ , of the transient current should reflect the energy relaxation time,  $\tau_r$ , from the ES to the GS.

We can relate  $\tau$  and  $\tau_r$  from the rate equation taking into account all the tunneling processes shown schematically in Fig. 1(c) [10,11]. Taking  $j_L \gg j_R$  and  $1/\tau < j_{L,e} + j_{L,g}$  (valid for measurable current), the

average number of tunneling electrons during one period of the pulse,  $\langle n_e \rangle$ , is

$$\langle n_e \rangle = A j_{R:e} \tau (1 - e^{-t_h/\tau}); \quad (1)$$

where  $A = \frac{j_{L:e}}{j_{L:e} + j_{L:g}}$  is the injection efficiency into the ES. The decay time is obtained as

$$\tau = \tau_1 = \tau_2 + j_{R:e} (1 - A); \quad (2)$$

containing information about  $\tau_2$ . The second term arises from the sequential tunneling process, in which an electron first escapes from the ES to be followed by an electron tunneling into the GS.

In addition to the transient current, we can also measure the stable current through the GS as a reference. The ES and GS become empty during the low-phase of the pulse, and only the GS contributes to the stable current during the high-phase of the pulse. Because there is no current-blocking for the stable current, the average number of tunneling electrons,  $\langle n_g \rangle$ , should be

$$\langle n_g \rangle = j_{R:g} t_h; \quad (3)$$

### III. MEASUREMENTS ON A LATERAL QD

First, we study a lateral quantum dot, which is fabricated in an AlGaAs/GaAs modulation doped heterostructure by using focused ion beam implantation (dark horizontal lines in the secondary electron micrograph (SEM) image of Fig. 2(a)) and Schottky gates (bright vertical lines separated by 220 nm) [6,10,12,13]. The dot contains about  $N \gg 50$  electrons. The addition energy is about 2 meV and the single particle energy spacing is 100 - 300  $\mu$ eV. Since this device has multiple gates, some parameters can be changed independently by appropriately adjusting the gate voltages. We tune the two gate voltages,  $V_L$  and  $V_R$ , such that the tunneling rate of the left barrier,  $j_{L:}$ , is much larger than that of the right barrier,  $j_{R:}$ . Therefore, the incoming tunneling rate to the dot is larger than the outgoing tunneling rate at a positive bias voltage,  $V_b > 0$ , (for the polarity defined in Fig. 2(a)). We perform the following measurements at a temperature of 150 mK and in a magnetic field,  $B$ , applied perpendicular to the substrate.

We apply a square-like pulse waveform through a dc-block (low frequency cut off at 700 Hz) and a low-loss coaxial cable (about 3 m long with a loss of  $< 3$  dB for dc - 10 GHz). There is no termination near the sample, and the reflected pulse, as shown in Fig. 2(b), is more or less the actual pulse waveform at the gate. The rise time (about 0.2 ns) of the pulse is faster than  $j_{L:g}^{-1}$  (typically about 1 ns), so the GS is not immediately occupied. The pulse length,  $t_h$ , is varied from 10 ns to 10  $\mu$ s, and the average current is measured.

We investigate the transient and stable currents as a function of the pulse length,  $t_h$ . We can obtain the average number of tunneling electrons per pulse,  $\langle n_g \rangle$ , for the stable current through the GS, and  $\langle n_e \rangle$  for the transient current through the ES from the  $I(t_h + t_l) = e$  value for each peak current  $I$ . Figures 2(c) and (d) show the results for the same  $N$  but measured at slightly different magnetic fields [ $B = 1.19$  T for (c) and 1.35 T for (d)]. From the  $B$ -dependence of the excitation spectrum (not shown), the ESs show complicated crossing and anti-crossing behavior at around  $B = 1.3$  T, while the characteristic of the GS is unchanged for  $B = 1.1 - 1.5$  T [11]. The transient current observed in Fig. 2(c) and (d) originates from ESs with different characteristics. For both cases,  $\langle n_g \rangle$  depends linearly on  $t_h$ , indicating a continuous current flow. The slope of these traces,  $d\langle n_g \rangle/dt_h = j_{R:g} \gg (300 \text{ ns})^{-1}$ , are almost the same for two cases. For the transient current,  $\langle n_e \rangle$  shows saturation behavior, which appears at very different pulse lengths  $t_h$ . From fitting with a single exponential function (Eq. 1),  $\tau = (1 - e^{-t_h/\tau})^{-1}$ , we obtain the decay time  $\tau = 2.1 \mu$ s for  $B = 1.35$  T, and  $\tau = 2$  ns for  $B = 1.19$  T.

Next we have to evaluate Eq. 2, in order to obtain the relaxation time  $\tau_2$ . The second term,  $j_{R:e} (1 - A)$ , can be estimated from the dc current characteristics assuming  $j_{L:e} = j_{L:g} = j_{R:e} = j_{R:g}$ .  $j_{R:e} (1 - A) \gg (1.2 \mu\text{s})^{-1}$  is obtained for the two cases. Thus  $\tau_2 = 2.1 \mu$ s for  $B = 1.35$  T is determined by a sequential tunneling process, and the energy relaxation time of interest is longer than that; i.e.,  $\tau_2 > 2.1 \mu$ s. By contrast,  $\tau_2 = 2$  ns for  $B = 1.19$  T.

The significantly different relaxation times can be understood in terms of spin-conservation during relaxation. If the ES and GS have the same spin, the electron in the ES quickly relaxes to the GS as a result of fast electron-phonon interaction (typically about  $\tau_{e\text{-ph}} \gg 1$  ns) [8]. By contrast, if the ES and GS have different spins, the relaxation time is limited by spin-flip processes. Most of the spin relaxation mechanisms discussed for 3D or 2D electrons in GaAs are suppressed for 0D states of QDs. We expect an extremely long spin relaxation time ( $\tau_{\text{spin}} > 10 \mu$ s) due to the small spin-orbit interaction [9]. This is beyond our experimental limit (a few  $\mu$ s), and explains well the long-lived ESs we observe. In this case the long-lived ES should have different spins from that of the GS. In our experiment, the Zeeman splitting is small and unresolved. Thus it is the difference in the total spin that is responsible for the long energy relaxation time, and for the appearance of the transient current.

Assuming spin conservation during relaxation, the pulse excitation technique is useful to analyze the excitation spectrum inside a QD. On application of a square pulse ( $t_h = t_l$ ), the amplitude of the net transient current,  $I_e$ , is given by

$$I_e = \hbar n_e i e = (t_h + t_l) = \frac{1}{2} e A_{j_R;e} \zeta^{\pm} = t_h (1 \mp e^{i t_h = \zeta^{\pm}}): \quad (4)$$

This can be approximated to  $I_e = \frac{1}{2} e A_{j_R;e}$  for  $\zeta^{\pm} \gg t_h$ , and  $I_e = \frac{1}{2} e A_{j_R;e} \zeta^{\pm} = t_h$  for  $\zeta^{\pm} \ll t_h$ . Thus, the transient current decreases, if the pulse length,  $t_h$ , is made much longer than  $\zeta^{\pm}$ . The transient current  $I_e$  for the two cases presented above (kept at a 20% duty ratio,  $t_h = (t_h + t_l) = 0.2$ ) is plotted in Fig. 2(e). The solid line is a fitting curve using Eq. 4. With an appropriate value of  $t_h$  ( $\zeta_{\text{eph}} \ll t_h < \zeta_{\text{spin}}$ ), the transient current appears for an ES whose total spin is different from that of any lower lying state. This technique is useful for studying the spin-dependent energy relaxation described in the next section, and other spin-dependent phenomena in QDs.

#### IV. MEASUREMENTS ON A VERTICAL QD

We also perform transient current spectroscopy on a vertical QD (artificial atom), in which the total number of electrons,  $N$ , and total spin,  $S$ , are well defined [24]. Electrons are confined by an approximate 2D harmonic potential (confining energy  $\sim 4$  meV). The  $N$ -dependent addition energy,  $E_a = 2 - 5$  meV, clearly reveals a shell structure for sequential electron filling. Interacting electrons inside the dot form many-body states well characterized by total spin,  $S$ , and total angular momentum,  $M$ . These quantum numbers can be identified from the magnetic field (applied parallel to the current),  $B$ , dependence of the single-electron tunneling current spectrum. Zeeman splitting is not resolved in this measurement so we neglected it.

The QD is weakly coupled to the top and bottom electrodes via asymmetric barriers. Figure 3(b) is the conventional dc excitation spectrum (the color represents the amplitude of  $dI/dV$ ) obtained for a dc bias voltage of  $V_b = -1.5$  mV. The  $n$ -th current stripe starting from the most negative  $V_g$  gives information about the tunneling transition between the  $N = n - 1$  and  $N = n$  electron system. The negative bias polarity is chosen such that an electron is injected through the thicker top tunneling barrier ( $\tau_{\uparrow} \gg 100$  ns) and ejected through the thinner bottom tunneling barrier ( $\tau_{\downarrow} \gg 10$  ns). The current increases in a step-like manner (positive peak appears in  $dI/dV$ ) when  $N$ -electron energy states enter the transport window, and decreases (negative peak in  $dI/dV$ ) when energy states leave the transport window. The positive-peak positions for  $n = 1 - 3$  are traced in Fig. 3(d). We can identify these states by comparison with an exact diagonalization calculation [14]. The identified quantum numbers  $(N; S; M)$  are labeled in Fig. 3(d). For the second stripe ( $n = 2$ ), in which the  $N = 2$  electron energy spectrum appears, a transition from the spin-singlet state  $(N; S; M) = (2; 0; 0)$ , which has anti-parallel spin electrons in the lowest orbital, to

spin-triplet state  $(N; S; M) = (2; 1; 1)$ , which has spin-polarized electrons in the lowest two different orbitals, appears at  $B = B_{S_{\uparrow\downarrow}} \gg 5$  T. Similarly,  $(N; S; M)$  can be identified for higher  $N$ .

For transient current spectroscopy, a small positive dc bias voltage  $V_b = 0.15$  mV is applied in such a way that an electron is injected through the thinner bottom barrier, and ejected through the thicker top barrier. A square pulse is applied in the same way as described in the previous section [see Fig. 3(a)]. Since the QD is fabricated on a conducting GaAs substrate, the parasitic capacitance of the gate electrode (mainly for bonding pad area) degrades the rise time of the pulse to 1 - 3 ns. This is comparable to the transport timescale ( $\tau_{\text{tot}}^{-1} \sim (\tau_{\text{b}} + \tau_{\text{t}})^{-1} \gg 10$  ns) of the dot, and the amplitude of the transient current is smaller than expected. However, we still see a clear transient current signal. In the following experiment, the pulse length ( $t_h = t_l = 300$  ns) is chosen to be much longer than  $\zeta_{\text{eph}} \gg 1$  ns but smaller than  $\zeta_{\text{spin}} > 10$  ns, so that a transient current appears only for long-lived ESs whose total spin is different from that of lower-lying states. The  $B$ -dependence of the transient current spectrum is shown in Fig. 3(c). The pair of peaks at the upper and lower edge of the  $n$ -th current stripe is due to transport through the  $N = n$  electron GS. The transient current through the same  $N$  ESs appears within the stripe. The singlet-triplet transition for  $N = 2$  is clearly seen at  $B = B_{S_{\uparrow\downarrow}}$ . Transient current is observed for the triplet ES when  $B < B_{S_{\uparrow\downarrow}}$ , and for the singlet ES when  $B > B_{S_{\uparrow\downarrow}}$ , since relaxation in both cases requires a spin-flip.

We measure the decay time  $\zeta^{\pm}$  of the transient current by changing the pulse length. As is the case for the lateral QD, clear saturation behavior is observed (not shown). The obtained decay time  $\zeta^{\pm} = 50$  ns - 1 ns, depending on the magnetic field, spin states, and samples, is always determined by sequential tunneling processes (the second term in Eq. 1). The spin-flip energy relaxation time  $\zeta$  is beyond the measurable range for this technique, but we can conclude that  $\zeta$  is longer than the typical transport timescale ( $\tau_{\uparrow}^{-1}$ ).

From the  $n = 3$  stripe, we can see some ESs which can relax to the GS without a spin-flip. The ES  $(N; S; M) = (3; \frac{1}{2}; 1)$  appearing in the dc excitation spectrum at  $B = 0 - 1$  T, is absent in the transient current. Since the  $N = 3$  GS is  $(N; S; M) = (3; \frac{1}{2}; 1)$  at this field, energy relaxation takes place immediately without a spin-flip. Similarly, some ESs at around 5 T are missing in the transient current [see Fig. 3(d)]. We do not see any transient current ( $< 50$  fA) for these states even when the pulse length is reduced to  $t_h = t_l = 20$  ns (further reduction of the pulse length induces non-resonant pumping). The absence of the transient signal implies that the relaxation time  $\zeta_{\text{eph}}$  is shorter than  $\gg 10$  ns.

One can see additional differences between the dc and pulse excitation spectrum. The dc excitation spectrum

has many extra weak features, which do not show any clear B-dependence. These can originate from weak modulation of the density of state in the top electrode, since its volume is so small [ $\gg (0.5 \text{ nm})^3$ ] [4,5]. These features are suppressed in the transient current spectrum, because the transport is allowed only when an ES is located in the small transport window [see Fig. 1(c)]. However, we see weak modulation in the amplitude of the transient current, although this is not clear for the color scale used in Fig. 3(c).

## V. SUMMARY

In summary, pulse excitation measurements are ideal for the investigation of energy relaxation times inside a QD. For an appropriate pulse length, we can obtain the energy spectrum for only long-lived ESs, which have different total spin from that of lower-lying states. We find that the spin-flip energy relaxation time is longer than the typical transport timescale, and that spin-conservation provides a selection rule for the energy-relaxation in GaAs QDs.

- 
- [1] For a review, see L. P. Kouwenhoven et al., in "Mesoscopic Electron Transport" ed. L. L. Sohn, L. P. Kouwenhoven, and G. Schön, NATO ASI series E 345, pp. 105-214.
  - [2] L. P. Kouwenhoven et al., Reports on Progress in Physics 64, 701 (2001).
  - [3] S. Tarucha et al., Phys. Rev. Lett. 77, 3613 (1996).
  - [4] L. P. Kouwenhoven et al., Science 278, 1788 (1997).
  - [5] S. Sasaki et al., Nature 405, 764 (2000).
  - [6] T. Fujisawa et al., Science 282, 932 (1998).
  - [7] T. Fujisawa et al., Physica E. 7, 413 (2000).
  - [8] U. Bockelmann, Phys. Rev. B 50, 17271 (1994).
  - [9] A. V. Kaetskii and Yu. V. Nazarov, Phys. Rev. B 61, 12639 (2000), cond-mat/0003513.
  - [10] T. Fujisawa et al., Phys. Rev. B 63, 081304(R) (2001).
  - [11] T. Fujisawa et al., Physica B 298, 573 (2001).
  - [12] T. H. Oosterkamp et al., Nature 395, 873 (1998).
  - [13] T. Fujisawa et al., Appl. Phys. Lett. 68, 526 (1996).
  - [14] S. Tarucha et al., Physica E 3, 112 (1998).

## Figure captions

Fig. 1. (a) Schematic time-dependent gate voltage,  $V_G(t)$ , used to obtain the transient current signal. (b) Schematic energy diagram when the pulse is in the low-phase for depletion. Both the excited state (ES) and the ground state (GS) become empty.  $\mu_L$  and  $\mu_R$  are the chemical potential of the left and right contact, respectively. (c) Schematic energy diagram when the pulse is in the high-phase for transient transport and relaxation. The transient current through the ES continues until the GS is occupied.

Fig. 2.(a) Schematic setup for the pulse measurements. The SEM picture is of the lateral quantum dot used in this study. The measurements are performed at a temperature of 150 mK in a magnetic field,  $B = 0 - 2 \text{ T}$ , perpendicular to the substrate. (b) Typical pulse waveform obtained by time-domain reflectometry. (c) and (d) Average number of tunneling electrons per pulse period through a GS ( $\langle n_{gi} \rangle$ , open symbols) and through the same N ES ( $\langle n_{ei} \rangle$ , filled symbols). (c) is obtained at  $B = 1.35 \text{ T}$  and (d) is obtained at  $B = 1.19 \text{ T}$  for the same N electron QD. (e) Transient current amplitude for  $B = 1.19 \text{ T}$  (solid circles) and  $1.35 \text{ T}$  (open circles).  $\tau$  is the characteristic decay time discussed in the text.

Fig. 3 (Color). (a) Schematic setup for the vertical quantum dot measurement. The measurements are performed at a temperature of 50 mK in a magnetic field,  $B = 0 - 8 \text{ T}$ , perpendicular to the substrate (parallel to the current). (b) Magnetic field dependence of the dc excitation spectrum obtained with  $V_b = -1.5 \text{ mV}$ . The color represents the amplitude of  $dI/dV$  [blue for negative, white for zero, and red for positive values]. Positive peaks in the n-th current stripe correspond to electron injection into GS and ESs of the  $N = n$  electron QD. (c) Magnetic field ( $B$ ) dependence of the transient current spectrum for  $V_p \gg 55 \text{ mV}$  and  $t_h = t_l = 300 \text{ ns}$ . The color represents the current amplitude [blue(-0.05 pA) - white/yellow ( $\gg 0 \text{ pA}$ ) - red (0.1 pA) - black (0.2 pA)]. The negative current is from non-resonant pumping. The arrow ( $B = B_{S_i \uparrow}$ ) indicates singlet-triplet transition for 2-electron QD. (d) Position of peaks from dc excitation spectrum. The lines are deduced from (b). The numbers in the figure represent the total spin,  $S$ , the total angular momentum,  $M$ , of ( $N = n$ )-electron states. The red (black) lines are the states which appear (do not appear) in the pulse-excited current spectrum of (c).

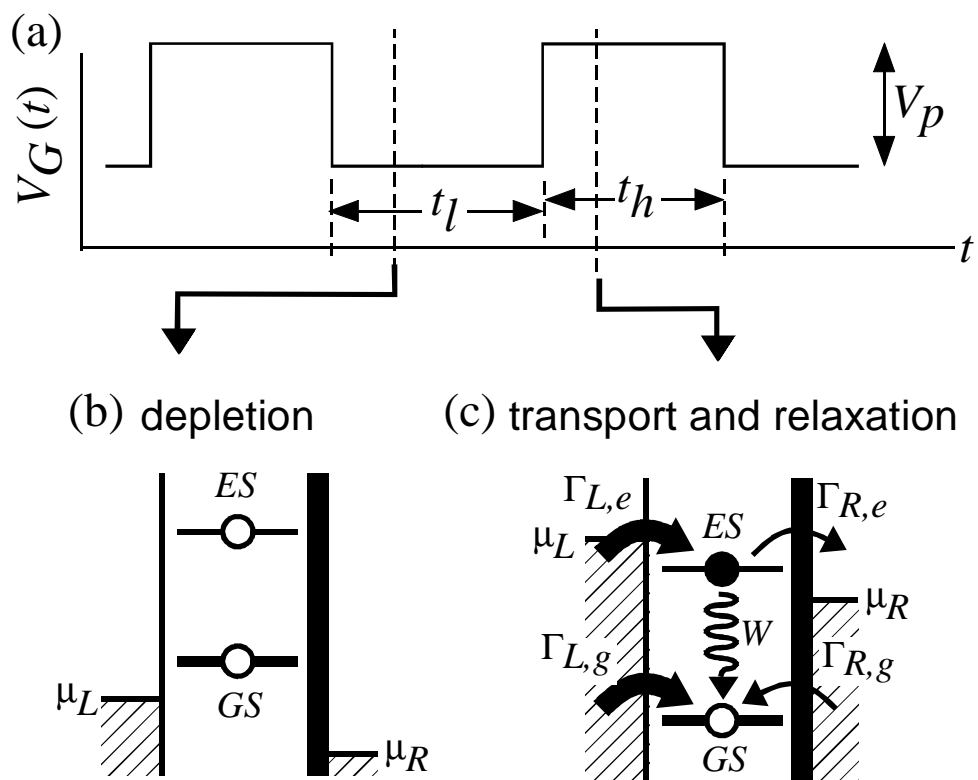


Fig. 1 of 3. T. Fujisawa et al.

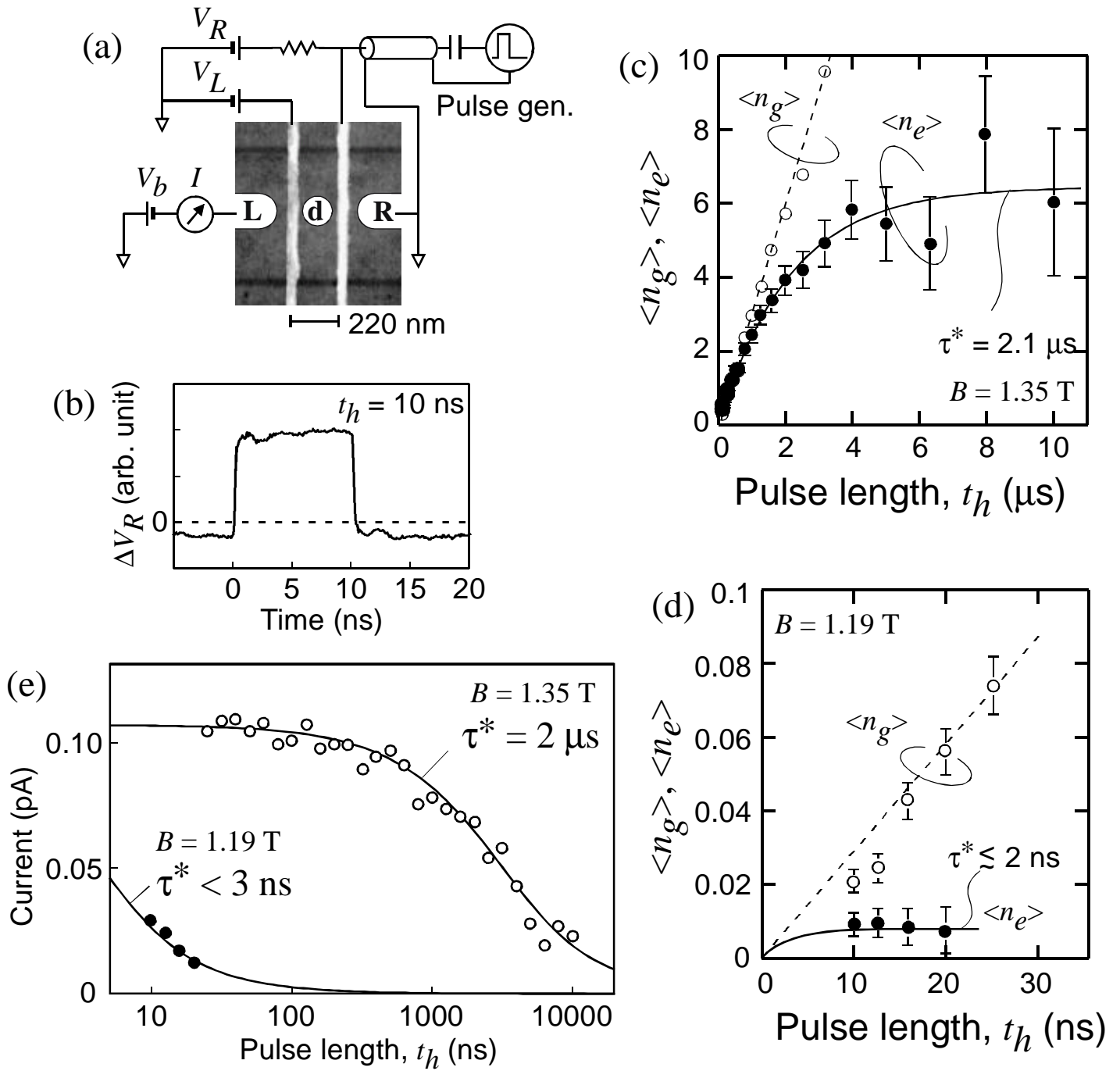


Fig. 2 of 3. T. Fujisawa et al.

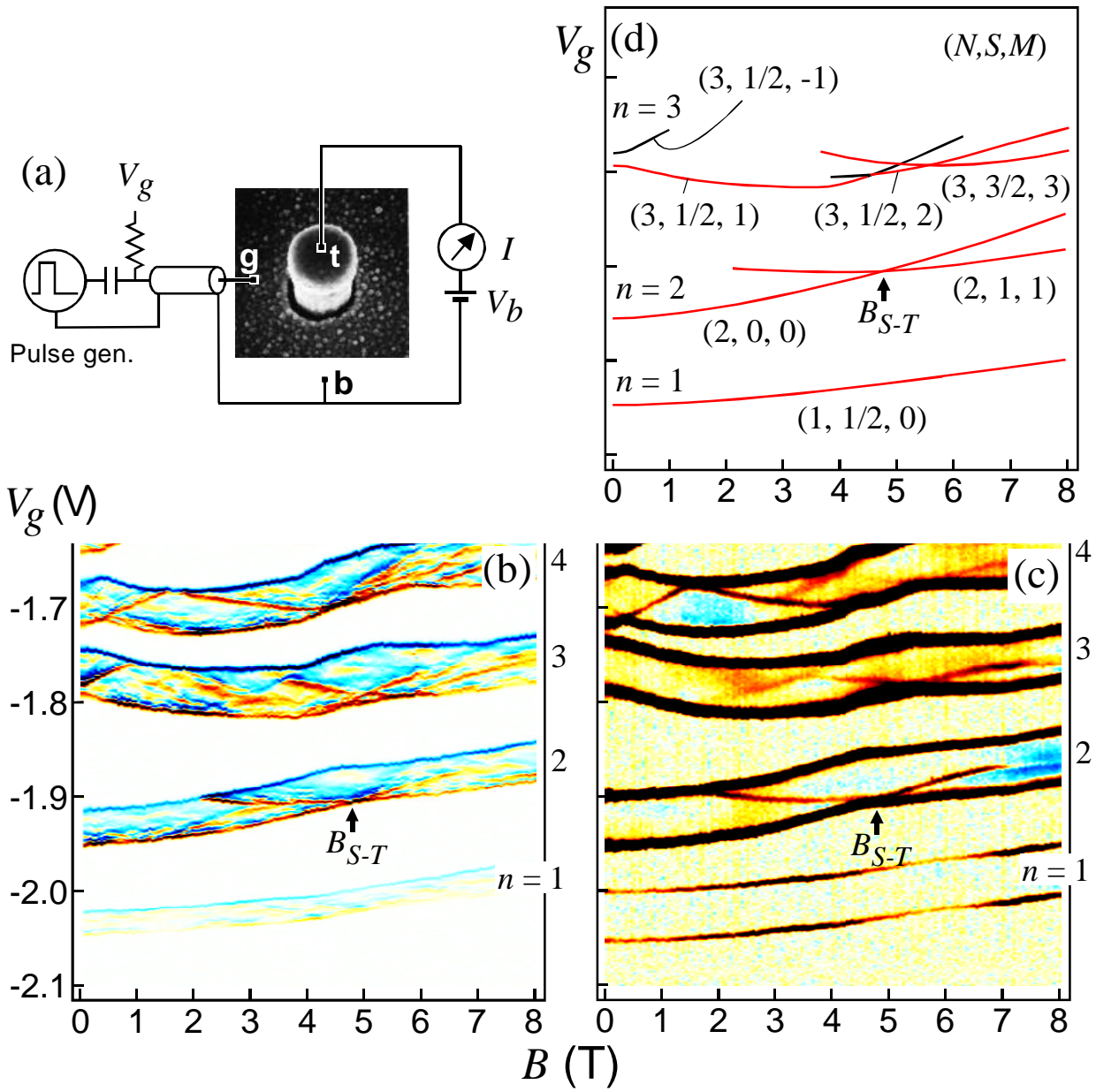


Fig. 3 of 3.(Color) T. Fujisawa et al.